Contents lists available at ScienceDirect

Physics and Imaging in Radiation Oncology

Original Research Article

The accuracy of artificial intelligence deformed nodal structures in cervical online cone-beam-based adaptive radiotherapy

Ethan Wang, Allen Yen, Brian Hrycushko, Siqiu Wang, Jingyin Lin, Xinran Zhong, Michael Dohopolski, Chika Nwachukwu, Zohaib Iqbal, Kevin Albuquerque *

University of Texas Southwestern Medical Center, Department of Radiation Oncology, Dallas, TX, United States

ARTICLE INFO

ABSTRACT

Background and Purpose: Online cone-beam-based adaptive radiotherapy (ART) adjusts for anatomical changes during external beam radiotherapy. However, limited cone-beam image quality complicates nodal contouring. Despite this challenge, artificial-intelligence guided deformation (AID) can auto-generate nodal contours. Our study investigated the optimal use of such contours in cervical online cone-beam-based ART.
Materials and Methods: From 136 adaptive fractions across 21 cervical cancer patients with nodal disease, we extracted 649 clinically-delivered and AID clinical target volume (CTV) lymph node boost structures. We assessed geometric alignment between AID and clinical CTVs via dice similarity coefficient, and 95% Hausdorff distance, and geometric coverage of clinical CTVs by AID planning target volumes by false positive dice. Coverage of clinical CTVs by AID contour-based plans was evaluated using D100, D95, V100%, and V95%.
Results: Between AID and clinical CTVs, the median dice similarity coefficient was 0.66 and the median 95 % Hausdorff distance was 4.0 mm. The median false positive dice of clinical CTV coverage by AID planning target volumes was 0. The median D100 was 1.00, the median D95 was 1.01, the median V100% was 1.00, and the median V95% was 1.00. Increased nodal volume, fraction number, and daily adaptation were associated with reduced clinical CTV coverage by AID-based plans.
Conclusion: In one of the first reports on pelvic nodal ART, AID-based plans could adequately cover nodal targets. However, physician review is required due to performance variation. Greater attention is needed for larger, daily-adapted nodes further into treatment.

1. Introduction

External beam radiotherapy (EBRT) is a primary treatment for locally advanced cervical cancer [1]. However, treatment planning is complicated by anatomical variation over the treatment course due to differences in bladder filling and rectal gas between fractions [2,3]. Additionally, an EBRT course typically spans 25–28 fractions over five weeks [1], allowing for longitudinal anatomic changes associated with tumor regression and weight fluctuation [4]. Rigid treatment planning may result in inadequate tumor coverage and increased normal structure toxicity [4].

Online adaptive radiotherapy (ART), which uses day-of-treatment imaging for re-contouring and re-planning, can account for these anatomical changes [4]. Specifically, online cone-beam-based ART, a subset of online ART using cone-beam computed tomography (CBCT) for rapid image acquisition, has proven clinically feasible for treating

cervical cancer [5,6]. Accurately delineating nodes within a reasonable timeframe is crucial for patient comfort and to limit intra-fraction motion [7], and the re-contouring of simultaneously treated lymph node boost structures is especially time-consuming and difficult due to their small size, high quantity, and the limited image quality of CBCT images [8–11]. While MRI improves nodal visibility compared to CBCT, prolonged image acquisition time and smaller treatment field limits workflow efficiency and target coverage in MR-guided ART [12,13]. Ensuring adequate coverage of CTV lymph node boost structures is critical, as lymph node irradiation significantly improves response rates and overall survival in cervical cancer [14,15].

Although numerous studies have assessed the efficacy of pelvic malignancy auto-segmentation, evaluation of pelvic nodal auto-segmentation is infrequent [16]. Existing approaches have included a region-based segmentation algorithm centered on pixel similarity [17], convolutional neural network-based segmentation [18–20], and a deep

---

* Corresponding author at: 2280 Inwood Road, United States.
E-mail address: Kevin.Albuquerque@UTSouthwestern.edu (K. Albuquerque).

reinforcement learning model for region isolation prior to convolutional neural network-guided contour delineation [20]. Nonetheless, only Archambault and colleagues have established a method specific to online cone-beam CT and the ART workflow, achieving nodal contouring via deformable image registration of planning CT contours to day-of-treatment CBCTs using a predetermined set of OAR contours, or influencer structures, generated by pre-trained convolutional neural networks [21]. Adopting these artificial intelligence (AI) influenced, deformable image registration generated (AID) contours with minimal revision could reduce treatment time, enhancing patient comfort and minimizing intra-fractional motion. Current literature has established that AID contours effectively delineate both organs at risk (OAR) and target volumes and can be used to generate plans with sufficient target coverage [22,23,5,6]. Yet, a focused assessment of the clinical feasibility of nodal AID contours has not yet been performed.

Our study thus aims to build on existing research by determining the clinical feasibility of AID nodal contours in cervical online cone-beam-based ART by assessing the coverage of clinical CTV lymph node boost structures by AID contour-based plans and the geometric overlap between AID and clinical CTV lymph node boost contours. By examining how AID contour performance varies over time, with daily patient status, and with nodal characteristics, we also aimed to characterize factors influencing AID contour performance, thereby informing clinicians on when AID contours should be employed.

2. Materials and methods

2.1. Patient selection and demographics

From our institutional ART Registry, we identified cervical cancer patients requiring pelvic, *para*-aortic, and/or inguinal gross nodal boost and receiving one or more fractions of online cone-beam-based ART from 9/17/2021 to 1/2/2023. Demographic data was obtained on patient age and FIGO stage. This study received approval from the Institutional Review Board at UT Southwestern Medical Center (Approval number: 082013–008).

All 21 patients had node positive tumors and received definitive chemoradiotherapy. Nineteen patients received simultaneous integrated boost, while two patients received sequential boost. Nineteen patients received high dose-rate brachytherapy following EBRT. Two patients did not receive high dose-rate brachytherapy following EBRT due to elimination of disease not confined to the *para*-aortic lymph nodes in a prior treatment course and poor tolerance of EBRT respectively. Two stage IIIC1 patients receiving definitive chemoradiotherapy for limited nodal groin disease and one stage IIB patient with recurrent *para*-aortic disease were included in the study (Table 1). The median unique nodal count per patient was 4.0 (IQR: 3.5).

2.2. Online cone-beam-based ART workflow

In the Varian Ethos (Varian Medical Systems, Palo Alto, CA) online cone-beam-based ART workflow (Supplementary Figure 1), a CT simulation was performed, followed by generation of a "scheduled plan," or baseline treatment plan that could be rigidly translated to later fractions, by dosimetrists. Each fraction, a CBCT was obtained, and two sets of CTV and OAR simulation CT structures were generated on the CBCT: One set via rigid propagation of simulation CT contours to the CBCT, and a second set via AI-guided deformation of CT simulation contours to the CBCT. For each structure, either the rigidly propagated or AID contours were selected as a starting point, final edits were made by the treating physician to produce "clinical contours," and an "adapted plan" was generated in Ethos based on the clinical contours and treatment goals. The initial AID contours for all structures were also stored in the system alongside correspondingly created adapted plans [24]. Nodal boost contouring was conducted in concordance with EMBRACE II guidelines [25].

Table 1
Patient characteristics at EBRT initiation.

N = 21		
FIGO Stage		
	IIB	1
	IIIA	1
	IIIB	1
	IIIC1	11
	IIIC2	4
	IVA	3
Age (years) at EBRT start		
	Median	46
	Range	29–68
Adaptation Scheme*		
	Daily	7
	Weekly	3
	Bi-Weekly	1
	On-Demand	10

*Daily: scheduled adaptation for all fractions. Weekly: scheduled adaptation each week. Bi-Weekly: scheduled adaptation twice a week. On-Demand: adaptation per clinical judgement. Adaptation scheme was based on clinician judgement regarding expected tumor response, weight changes, and response to prior fractions.

2.3. Contour and plan extraction

For all adaptive fractions from each patient, clinical and AID CTV and planning target volume (PTV) lymph node boost structures were extracted from DICOM data stored in an institutional database, allowing for assessment of the evolution of nodal structures over treatment. The CTV to PTV margin was 5 mm. Partitioning was performed for initially extracted structures containing multiple nodes to facilitate discrete analysis of individual nodes. Clinical and AID-based plans were extracted for all included fractions well. DICOM processing, contour extraction, contour partitioning, and plan extraction were performed using RT-Utils 0.0.6 [26], dicompyler 0.4.2 [27], Hungarian assignment [28], and SciPy 1.10 [29] in Python 3.11.2 [30], and is further described in the Supplemental Methodology.

We extracted 104 unique CTV lymph node boost structures from 21 patients across 136 total fractions—649 structures total. Each unique CTV lymph node boost structure occurred in an average of 6.2 fractions (SD = 6.0). Sequential boost was delivered to 7 % of CTV lymph node boost structures, while 75 % received simultaneous integrated boost. The majority of CTV lymph node boost structures were from daily adapted patients 64 %, with 64 % being upper pelvic, 20 % lower pelvic, 12 % *para*-aortic, and 4 % inguinal. The median clinical volume of CTV lymph node boost structures on CBCT was 1.8 cm^3(IQR: 1.0–5.4cm^3), with a mean prescribed dose of 57.5 Gy (SD: 2.1 Gy).

2.4. Evaluating contour quality

To assess geometric overlap between AID and clinical CTV lymph node boost structures, the volumetric dice similarity coefficient, false positive dice, false negative dice, and 95 % Hausdorff distance were computed from the relevant binary masks using DeepMind's surface-distance library [31] (Supplemental Figure 2C). Geometric coverage with expanded margins was evaluated via calculation of the false positive dice of clinical CTV lymph node boost structures relative to associated AID PTV structures. To evaluate the acceptability of AID coverage, the dose distribution of the adapted plan generated from AID contours were overlaid on clinical CTV lymph node boost contours. D100 (Gy/prescription dose), D95 (Gy/prescription dose), V100%, and V95% were then computed. Clinical volume on CBCT, location, intrafraction nodal count, fraction number, and daily patient status were obtained for each CTV lymph node boost structure for stratification of nodal metrics.

2.5. Statistical analysis

Univariate analyses were performed to assess the influence of stratifying factors on clinical CTV coverage by AID-based plans and geometric performance, and subsequent multivariate regressions including significant or near-significant factors ($p <= 0.1$) from univariate analyses were then performed. Change in clinical nodal volumes by fraction was assessed as well. Statistical analyses were performed using Python 3.11.2 [30], Scipy 1.10.1 [29], and Statsmodels 0.13.5 [32] in Jupyter Notebook 6.4.12 [33]. Additional detail on acquisition of descriptive statistics and statistical test selection is described in the Supplemental Methodology.

To determine whether instances of poor AID to clinical CTV lymph node boost alignment were attributable to inaccuracy of the clinical or AID contour, CTV lymph node boost structures with an AID to clinical 95 % Hausdorff distance > 30 mm were visually assessed by three of the co-authors.

3. Results

For AID plan coverage of clinical CTV lymph node boost structures, median D100 was 1.00 (IQR:0.05), median D95 was 1.01 (IQR:0.02), median V100% was 1.00 (IQR:0.04), and median V95% was 1.00 (IQR:0). With dose from AID contour-based plans, a D100 > 95 % was attained in 76 % of CTV lymph node boost structures, and a D95 > 95 % was attained in 85 % of CTV lymph node boost structures (Fig. 1A). Distribution of clinical dose over clinical CTV lymph node boost

structures is shown in Fig. 1B for reference.

Geometric AID to clinical CTV lymph node boost structure comparisons revealed a median dice similarity coefficient of 0.66 (IQR:0.37 mm), median false positive dice of 0.27 (IQR:0.37 mm), median false negative dice of 0.42 (IQR: 0.44 mm), and median 95 % Hausdorff distance of 4.0 mm (IQR: 4.2 mm) (Fig. 1C). A median false positive dice of 0.00 (IQR: 0.01 mm) was obtained when comparing clinical CTV lymph node boost structures to AID PTV lymph node boost structures expanded 5 mm from AID CTVs. Across all dose and geometric metrics, AID CTV lymph node boost contours performed worse than clinical contours ($p << 0.01$) (Supplementary Table 1).

Univariate analyses for dose and geometric metrics are included in Supplementary Tables 2-5. In multivariate analysis, daily adaptation, increased fraction number, and larger clinical nodal volume on CBCT were significantly associated with reduced clinical CTV coverage by AID-based plans (Table 2), though clinical nodal volume demonstrated mixed geometric performance (Supplementary Table 6). Increased fraction number was associated with decreased clinical CTV lymph node boost volume (Spearman rho: −0.03), but this trend was not significant ($p = 0.43$).

The clinical vs. AID contour 95 % Hausdorff distance was > 30 mm in 3.7 % of CTV lymph node boost structures, revealing instances of significant spatial discrepancy. Qualitative assessment determined that inaccuracy of the AID contour was responsible for the extreme dissimilarity in all 24 cases of high 95 % Hausdorff distances. One instance of poor AID nodal detection is illustrated in Fig. 2. Additionally, AID contours often overlooked entire slices of clinical CTV lymph node boost
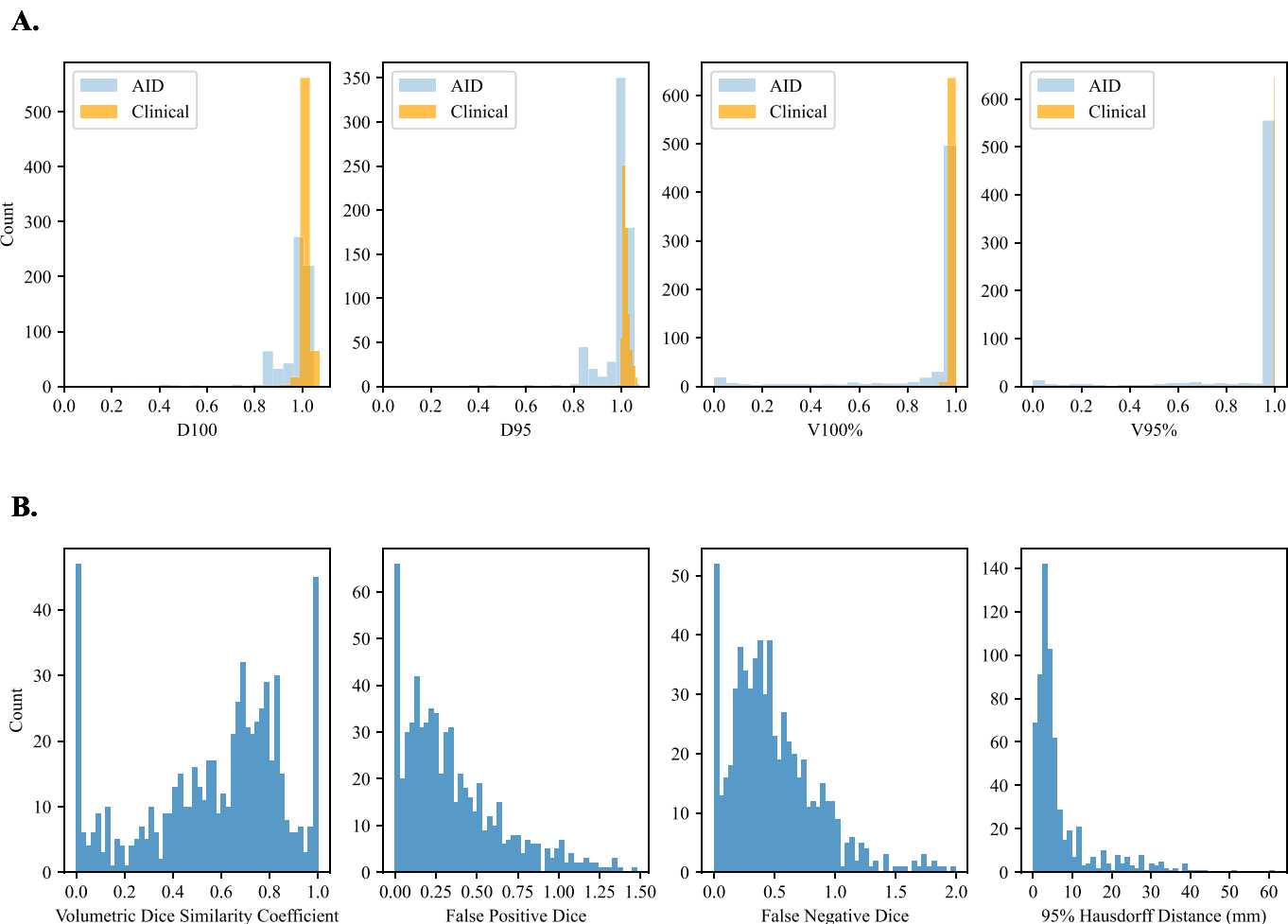
A.

B.

Fig. 1. A. Histogram plots showcasing distribution of AID and clinical dose over clinical CTV LNbst structures. B. Histogram plots showcasing distribution of metrics from geometric comparison of AID vs. clinical CTV lymph node boost structures.

Table 2

Robust (Huber) regression evaluating multivariate effect of stratifying factors on AID-based plan coverage of CTV nodal contours. * denotes significance.

Variable	D100		D95	
	Coefficient	P-value	Coefficient	P-value
Intercept	1.02	<<0.01*	1.02	<<0.01*
Inguinal	0.01	0.13	0.01	0.04
Para-Aortic	−0.01	0.06	−0.01	0.02
Lower-Pelvic	<<0.01	0.01	-<0.01	0.02
Upper Pelvic	reference	reference	reference	reference
Daily Status	−0.01	<0.01*	−0.01	<<0.01*
Intra-fraction Nodal Count	NI	NI	NI	NI
Clinical Volume	-<0.01	<<0.01*	-<<0.01	<<0.01*
Fraction Number	-<<0.01	<<0.01*	-<<0.01	<<0.01*
Variable	V100%		V95%	
	Coefficient	P-value	Coefficient	P-value
Intercept	0.99	<<0.01*	1.00	<<0.01*
Inguinal	0.01	0.02	-<<0.01	0.02
Para-Aortic	-<0.01	0.66	-<<0.01	0.43
Lower-Pelvic	-<<0.01	0.94	-<<0.01	0.96
Upper Pelvic	reference	reference	reference	reference
Daily Status	-<0.01	0.20	-<<0.01	0.06
Intra-fraction Nodal Count	<<0.01	0.11	<<0.01	0.02
Clinical Volume	-<<0.01	<<0.01*	-<<0.01	<<0.01*
Fraction Number	-<<0.01	<<0.01*	-<<0.01	<<0.01*

*A Bonferroni correction was applied to the significance threshold (p = 0.05/ number of factors evaluated) for each multiple regression to account for multiple comparisons.

*Reference denotes reference category. Upper pelvic was selected as the reference location as it was the most common nodal location.

*NI denotes variables not included due to lack of significance or near-significance in univariate analysis.

contours in certain nodes, as shown in Structure 1 of Supplementary Fig. 2A.

4. Discussion

Simultaneous nodal target coverage during pelvic online cone-beam-based ART for cervical cancer is just being explored in the clinical space, and the validity of AI-deformed nodal contours is unproven. We have demonstrated that online cone-beam-based ART plans generated from unedited AID contours can provide reasonable clinical CTV lymph node boost coverage in many situations with a 5 mm PTV. However, nodal characteristics vary across patients, and treatment-related changes may affect the ability of AID contours to consistently identify true nodal position and volume.

Multiple nodal characteristics influence the clinical feasibility of AID contours. In multivariate analysis, coverage of clinical CTV lymph node boost structures by AID contour-based plans was significantly reduced in later fractions, larger nodes, and nodes from patients receiving daily adaptation. In these scenarios, significant difference between the simulation CT and day-of-treatment CBCT was likely due to pre-treatment expectation of tumor response and anatomic change over the course of treatment respectively. Greater image-to-image discrepancy presents a harder deformation task, potentially explaining the reduced AID performance. This effect was identified by Li et al. who found a reduction in deformable image registration-based segmentation performance over time in head and neck ART [34]. Moreover, poor anatomic visualization due to post-radiation inflammation and edema, which may progressively worsen with increasing radiation effects in later fractions, may further contribute to this trend [35].

While the American Association of Physicists in Medicine recommends a minimal tolerable structure-to-structure dice similarity coefficient of 0.8 to 0.9 for image registration, the median dice similarity coefficient across CTV lymph node boost structures was 0.66 [36]. This limited geometric performance may be attributable to the greater susceptibility of smaller structures, such as nodes, to translational shift [37,38]. Nonetheless, the 5 mm CTV to PTV expansion in the setting of a median AID to clinical CTV 95 % Hausdorff distance of 4.0 mm accounted for this poor geometric performance, resulting in full AID PTV coverage of clinical CTV lymph node boost structures in over half of studied nodes. However, AID-based plan coverage of clinical CTVs may have been insufficient with a reduced margin. Smaller clinical nodal volume on CBCT was associated with improved clinical CTV coverage by AID-based plans, which can be attributed to the statistically significant and linear relationship between nodal size and 95 % Hausdorff distance (Supplemental Table 6). Lastly, while intra-fractional motion is comparatively small with prior studies demonstrating a 1.2 mm average overall patient displacement over 15 min for supine patients, intra-fractional shift is a pertinent factor that may affect optimal CTV to PTV expansion [7].

It is additionally important to consider that variance in AID contour performance leads to the occasional generation of clinically unacceptable outlier contours (Fig. 2). Nonetheless, such nodes may be accounted for via rapid physician review due to their readily apparent inaccuracy. Physicians can also prevent detrimental contours by referencing the original planning CT contours from CT simulation or by utilizing rigid contour propagation, which has can be valuable in instances of poor nodal visibility or limited mobility relative to bone [23].

While multiple studies have evaluated AID contours in the setting of pelvic online cone-beam-based ART [22,23,5,6], Åström et al., was the only study to separately analyze the quality of nodal AID contours [23]. Similar to our study, Åström et al. assessed the geometric overlap between nodal AID and clinical contours and AID-based plan coverage of
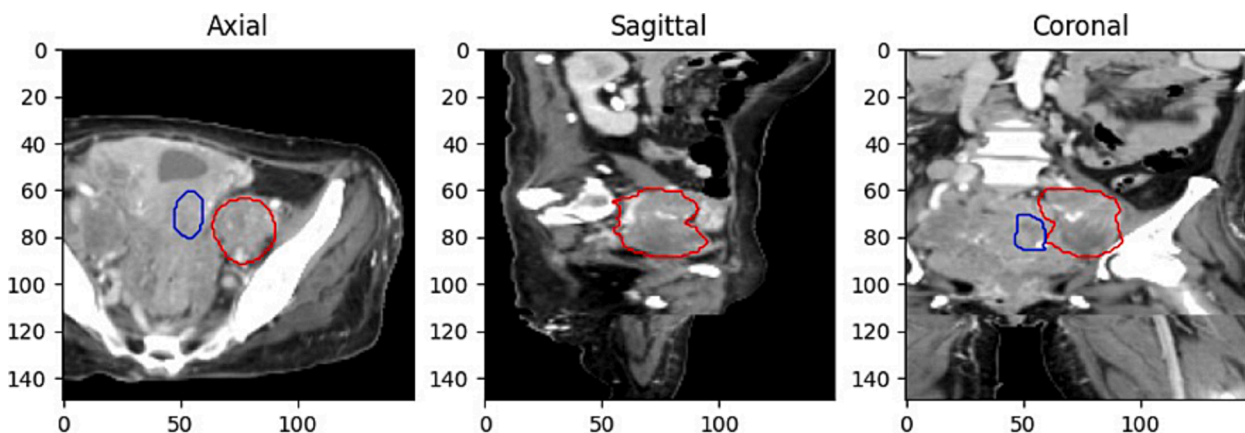

Fig. 2. An outlier CTV LNbst structure with poor AID to clinical CTV lymph node boost structure alignment (HD95 > 30 mm). Red = Clinical contour, Blue = AID contour. (For interpretation of the references to colour in this figure legend, the reader is referred to the web version of this article.)

nodal clinical contours. Yet, this analysis was limited to simulated treatment sessions, which do not capture the complexities and time-pressure of the clinical environment, pertained to anal as opposed to cervical online cone-beam-based ART, and treated nodal contours as single CTVs. Our novel DICOM processing method of delineating individual nodes from CTV structures encompassing multiple nodes allowed for an evaluation of individual node quality stratified by nodal characteristics, which has not yet been demonstrated in the literature. This information is essential to clinicians, as nodal AID contours are not uniformly accurate or inaccurate, and thus should not be invariably accepted or rejected. Identifying specific situations when AI-guided deformation is likely to be valuable thus provides clinicians with a more nuanced understanding of the optimal use of AID contours in clinical practice.

The clinical application of online cone-beam-based ART extends beyond cervical cancer, demonstrating effectiveness in pelvic malignancies such as prostate cancer, achieving sufficient PTV coverage with ~ 20 min treatment times [39] and generating AID nodal contours requiring no edits in most cases [40], and anal cancer, attaining reductions in OAR toxicity relative to non-adapted radiotherapy [23]. Online cone-beam-based ART has furthermore demonstrated feasibility in simulation-free palliative radiotherapy of thoracic, thoracic spinal, abdominal, lumbar spine/sacral, and pelvic treatment sites, highlighting its versatility [41]. Given uniformity in online cone-beam-based ART workflow across different clinical scenarios [42], our methodology of stratified nodal assessment may be widely applicable. Implementing this approach could enhance our understanding of AID nodal contouring in numerous treatment sites, mirroring the insights gained from our observations in cervical cancer.

Limitations of our study are as follows. First, clinical CTV lymph node boost contours were the gold standard for AID contour evaluation. However, the difficulty and time pressure of nodal contouring on CBCT may have produced sub-optimal clinical contours. Future improvements in CT hardware and reconstruction may alleviate this limitation. Second, in our workflow, AI-generated influencer structures were edited by radiation therapists prior to AID contour generation. 25 % of AI-influencer structures have been found to require major editing [22]. Thus, our findings may not generalize to workflows lacking human review of AI-generated influencer structures. Third, AID to clinical CTV lymph node boost comparisons assumed that the adaptive plan was selected for clinical delivery. This does not always occur. The adapted plan, which is re-optimized on day-of-treatment contours, or the scheduled plan, a translation of the pre-treatment plan onto day-of-treatment anatomy, can both be selected. Still, prior research indicates that the adapted plan is qualitatively superior in 88 % of cases [22]. Fourth, our study does not address the acceptability of rigidly propagated contours, which are often used as a baseline when nodes are difficult to visualize on CBCT, Fifth, plan-based coverage was based on both nodal and non-nodal AID contours, so the specific influence of AID lymph node boost contours as opposed to other target and OAR contours on clinical CTV lymph node boost coverage was not determined. Nonetheless, nodal structures are typically far apart from and minimally influenced by non-nodal structures. Sixth, the impact of AID-based plans on non-nodal clinical CTVs and OARs was not assessed. Lastly, minor issues arose in nodal analysis. We were unable separate discrete nodes if they were contoured within a single structure, and nodes with very small volumes presented issues with volume and dose calculation. Our nodal findings may additionally be biased by the large fraction (64 %) of nodal events from daily adapted patients.

In future studies, a more complete assessment of automated nodal contouring for online cone-beam-based ART can be achieved by investigating the quality of clinical contours, the acceptability of rigidly propagated contours, the importance of AI-influencer structure editing, and the effects of intra-fraction motion on nodal coverage. Investigating the clinical acceptability of nodal contours should also be performed with different margins, focusing on how margin reduction may improve

OAR toxicity while preserving CTV coverage. Lastly, we hope to build on our existing work by evaluating nodal coverage in non-cervical online cone-beam-based ART and in MR-based online adaptive radiotherapy.

In summary, unedited AID contours have the capacity to generate treatment plans with sufficient dose to most clinically defined nodal structures with a 5 mm margin. Thus, AID-generated contours may often serve as a viable starting point for contour editing. Nonetheless, instances of AID failure mandate at minimum a quick review of all unedited AID contours, and we further recommend that additional physician editing and attention be devoted to nodes that are larger, from later fractions, and from patients treated with daily adaptation.

CRediT authorship contribution statement

Ethan Wang: Conceptualization, Methodology, Software, Validation, Formal analysis, Investigation, Writing – original draft, Writing – review & editing. **Allen Yen:** Data curation, Conceptualization, Methodology, Writing – review & editing. **Brian Hrycushko:** Conceptualization, Methodology, Writing – review & editing. **Siqiu Wang:** Software, Writing – review & editing. **Jingyin Lin:** Data curation. **Xinran Zhong:** Conceptualization, Writing – review & editing. **Michael Dohopolski:** Software, Methodology, Writing – review & editing. **Chika Nwachukwu:** Writing – review & editing. **Zohaib Iqbal:** Supervision, Conceptualization, Methodology, Writing – review & editing. **Kevin Albuquerque:** Supervision, Conceptualization, Methodology, Resources, Writing – original draft, Writing – review & editing, Project administration.

Declaration of competing interest

The authors declare the following financial interests/personal relationships which may be considered as potential competing interests: As the authors of the manuscript, "To Deform or Not to Deform: The Accuracy of Artificial Intelligence Deformed (AID) Nodal Structures in Cervical Online Cone-beam Adaptive Radiotherapy (OnC-ART)", we declare the following conflicts of interest. Brian Hrycushko: Participating in Varian-sponsored clinical trial for cervical cancer. No funding provided. Kevin Albuquerque: Participating in Varian-sponsored clinical trial for cervical cancer. No funding provided. All other co-authors (Ethan Wang, Allen Yen, Siqiu Wang, Jingyin Lin, Xinran Zhong, Michael Dohopolski, Chika Nwachukwu, and Zohaib Iqbal) have no conflicts of interest to disclose. Thank you for considering our manuscript for publication.

Appendix A. Supplementary data

Supplementary data to this article can be found online at https://doi.org/10.1016/j.phro.2024.100546.

References

[1] ASTRO. ASTRO Guideline on Radiation Therapy for Cervical Cancer, https://www.astro.org/Patient-Care-and-Research/Clinical-Practice-Statements/Cervical-Cancer-Guideline; 2020 [accessed 6 December 2023].

[2] Dutta S, Dewan A, Mitra S, Sharma MK, Aggarwal S, Barik S, et al. Dosimetric impact of variable bladder filling on IMRT planning for locally advanced carcinoma cervix. J Egypt Natl Cancer Inst 2020;32:00033-5. https://doi.org/ 10.1186/s43046-020-00033-5.

[3] Berger T, Peterson JBB, Lindegaard JC, Fokdal LU, Tanderup L. Impact of bowel gas and body outline variations on total accumulated dose with intensity-modulated proton therapy in locally advanced cervical cancer patients. Acta Oncol 2017;(56):1472–8. https://doi.org/10.1080/0284186X.2017.1376753.

[4] Lim-Reinders S, Keller BM, Al-Ward S, Sahgal A, Kim A. Online Adaptive radiation therapy. Int J Radiat Oncol Biol Phys 2017;99:994-1003. https://doi.org/ doi: 10.1016/j.ijrobp.2017.04.023.

[5] Shelley CE, Bolt MA, Hollingdale R, Chadwick SJ, Barnard AP, Rashid M, et al. Implementing cone-beam computed tomography-guided online adaptive radiotherapy in cervical cancer. Clin Transl Radiat Oncol 2023;40:100596. https://doi.org/10.1016/j.ctro.2023.100596.

[6] Branco D, Mayadev J, Moore K, Ray X. Dosimetric and feasibility evaluation of a CBCT-based daily adaptive radiotherapy protocol for locally advanced cervical cancer. J Appl Clin Med Phys 2023;24:e13783.

[7] Hoogeman MS, Nuyttens JJ, Levendag PC, Heijmen BJ. Time dependence of intrafraction patient motion assessed by repeat stereoscopic imaging. Int J Radiat Oncol Biol Phys 2008;70:609–18. https://doi.org/10.1016/j.ijrobp.2007.08.066.

[8] Cai J, He X, Wang H, Dong W, Zhang Y, Zhao J, et al. Topographic distribution of lymph node metastasis in patients with stage IB1 cervical cancer: an analysis of 8314 lymph nodes. Radiat Oncol 2021;16:54. https://doi.org/10.1186/s13014-021-01781-x.

[9] Teng F, Yu H, Wang B, Yan Y, Gao C, Guo F, et al. Patterns of lymph node metastases and their implications in individualized radiotherapeutic clinical target volume delineation of regional lymph nodes in patients with endometrial cancer. J Cancer 2022;13:3575–83. https://doi.org/10.7150/jca.78009.

[10] Siewerdsen JH, Jaffray DA. Cone-beam computed tomography with a flat-panel imager: magnitude and effects of x-ray scatter. Med Phys 2001;(28):220–31. https://doi.org/10.1118/1.1339879.

[11] Endo M, Tsunoo T, Nakamori N, Yoshida K. Effect of scattered radiation on image noise in cone beam CT. Med Phys 2001;28:469–74. https://doi.org/10.1118/ 1.1357457.

[12] Winkel D, Kroon PS, Werenstejin-Honingh AM, Bol GH, Raaymakers BW, Jurgenliemk-Schulz IM. Simulated dosimetric impact of online replanning for stereotactic body radiation therapy of lymph node oligometastases on the 1.5T MR-linac. Acta Oncol 2018;57:1705–12. https://doi.org/10.1080/ 0284186X.2018.1512152.

[13] Werenstejin-Honigh AM, Kroon PS, Winkel D, Carlijn van Gaal J, Hes J, Snoeren LMW. Impact of magnetic resonance-guided versus conventional radiotherapy workflows on organ at risk doses in stereotactic body radiotherapy for lymph node oligometastases. Phys Imaging Radiat Oncol 2022;(30):66–73. https://doi.org/10.1016/j.phro.2022.06.011.

[14] Vargo JA, Kim H, Choi S, Sukumvanich P, Olawaiye AB, Kelley JL, et al. Extended field intensity modulated radiation therapy with concomitant boost for lymph node-positive cervical cancer: analysis of regional control and recurrence patterns in the positron emission tomography/computed tomography era. Int J Radiat Oncol Biol Phys 2014;90:1091–8. https://doi.org/10.1016/j.ijrobp.2014.08.013.

[15] Choi KH, Kim JY, Lee DS, Lee YH, Lee SW, Sung S, et al. Clinical impact of boost irradiation to pelvic lymph node in uterine cervical cancer treated with definitive chemoradiotherapy. Medicine (Baltimore) 2018;97:e0517.

[16] Kalantar R, Lin G, Winfield JM, Messiou C, Lalondrelle S, Blackledge MD, et al. Automated segmentation of pelvic cancers using deep learning: state-of-the-art approaches and challenges. Diagnostics (Basel) 2021;11:1964. https://doi.org/ 10.3390/diagnostics11111964.

[17] Debats OA, Litjens GJS, Barentz NK, Huisman HJ. Automated 3-dimensional segmentation of pelvic lymph nodes in magnetic resonance images. Med Phys 2011;38:6178–87. https://doi.org/10.1118/1.3654162.

[18] Rhee DJ, Jhingran A, Rigaud B, Netherton T, Cardenas CE, Zhang L, et al. Automatic contouring system for cervical cancer using convolutional neural networks. Med Phys 2020 Nov;47:5648–58. https://doi.org/10.1002/mp.14467.

[19] Zhao X, Xie P, Wang M, Li W, Pickhardt P, Xia W, et al. Deep learning-based fully automated detection and segmentation of lymph nodes on multiparametric-mri for rectal cancer: a multicenter study. EBioMedicine 2020;56:102780. https://doi.org/ 10.1016/j.ebiom.2020.102780.

[20] Rayn K, Gokhroo G, Jeffers B, Gupta V, Chaudhari S, Clark R, et al. Multicenter study of pelvic nodal autosegmentation algorithm of siemens healthineers: comaprison of male vs. female pelvis. Adv Radiat Oncol 2023;in press:101326. https://doi.org/ 10.1016/j.adro.2023.101326.

[21] Archambault Y, Boylan C, Bullock D, Morgas T, Peltola J, Ruokokoski E, et al. Making on-line adaptive radiotherapy possible using artificial intelligence and machine learning for efficient daily re-planning. Med Phys Intl Journal 2020;8: 77–86.

[22] Sibolt P, Andersson LM, Calmels L, Sjostrom D, Bjelkengren U, Geertsen P, et al. Clinical implementation of artificial intelligence-driven cone beam computed tomography-guided online adaptive radiotherapy in the pelvic region. Phys Imaging Radiat Oncol 2021;17:1–7. https://doi.org/10.1016/j.phro.2020.12.004.

[23] Åström LM, Behrens CP, Storm KS, Sibolt P, Serup-Hansen E. Online adaptive radiotherapy of anal cancer: normal tissue sparing, target propagation methods, and first clinical experience. Radiother Oncol 2022;176:92–8. https://doi.org/ 10.1016/j.radonc.2022.09.015.

[24] Varian. Ethos Algorithms Reference Guide 2019.

[25] Pötter R, Tanderup K, Kirisits C, de Leeuw A, Kirchheiner K, Nout R, et al. The EMBRACE II study: The outcome and prospect of two decades of evolution within the GEC-ESTRO GYN working group and the EMBRACE studies. Clin Transl Radiat Oncol 2018;9:48–60. https://doi.org/10.1016/j.ctro.2018.01.001.

[26] Shrestha A. RT-Utils, A minimal Python library for RTStruct manipulation, https:// pypi.org/project/rt-utils/0.0.6/; 2023 [accessed 6 December 2023].

[27] Dicompyler. Welcome to dicompyler, https://www.dicompyler.com/; 2014 [accessed 6 Decmeber 2023].

[28] Junger M, Liebling T, Naddef D, Nemhauser G, Pulleybank W, Reinelt G, et al. 50 Years of Integer Programming 1958–2008. 1st ed. Heidelberg: Springer, Berlin; 2010.

[29] SciPy. Project description, https://pypi.org/project/scipy/; 2023 [accessed 6 December 2023].

[30] Python. Python 3.11.2, https://www.python.org/downloads/release/python-3112/; 2023 [accessed 6 December 2023].

[31] Google Deepmind. Surface distance metrics, https://github.com/google-deepmind/surface-distance; 2022 [accessed 6 December 2023].

[32] Statsmodels. Statistical models, hypothesis tests, and data exploration, https:// www.statsmodels.org/v0.13.5/index.html; 2022 [accessed 6 December 2023].

[33] Jupyter Notebook. The Jupyter Notebook, https://jupyter-notebook.readthedocs. io/en/6.4.12/; 2023 [accessed 6 December 2023].

[34] Li X, Zhang YY, Shi YH, Zhou LH, Zhen X. Evaluation of deformable image registration for contour propagation between CT and cone-beam CT images in adaptive head and neck radiotherapy. Technol Health Care 2016;24:S747-55.24. https://doi.org/ 10.3233/THC-161204.

[35] Papadopoulou I, Stewart V, Barwick TD, Park WH, Soneji N, Rockall AG, et al. Post-radiation therapy imaging appearances in cervical carcinoma. Radiographics 2016; 36:538–53. https://doi.org/10.1148/rg.2016150117.

[36] Brock KK, Mutic S, McNutt TR, Li H, Kessler ML. Use of image registration and fusion algorithms and techniques in radiotherapy: Report of the AAPM Radiation Therapy Committee Task Group No. 132. Med Phys 2017;44:e43-e76. https://doi. org/10.1002/mp.12256.

[37] Shamir RR, Duchin Y, Kim J, Sapiro G, Harel N. Continuous dice coefficient: a method for evaluating probabilistic segmentations. Arxiv 2018.

[38] Rohlfing T. Image similarity and tissue overlaps as surrogates for image registration accuracy: widely used but unreliable. IEEE Trans Med Imaging 2012; 31(2):153–63. https://doi.org/10.1109/TMI.2011.2163944.

[39] Zwart LGM, Ong F, Ten Asbroek LA, van Dieren EB, Koch SA, Bhawanie A, et al. Cone-beam computed tomography-guided online adaptive radiotherapy is feasible for prostate cancer patients. Phys Imaging Radiat Oncol 2022;22:98–103. https:// doi.org/10.1016/j.phro.2022.04.009.

[40] Byrne M, Archibald-Heeren B, Hu Y, Teh A, Beserminji R, Cai E, et al. Varian ethos online adaptive radiotherapy for prostate cancer: early results of contouring accuracy, treatment plan quality, and treatment time. J Appl Clin Med Phys 2022; 23:e13479.

[41] Kejda A, Quinn A, Wong S, Lowe T, Fent I, Gargett M, et al. Evaluation of the clinical feasibility of cone-beam computed tomography online adapaptation for simulation-free palliative radiotherapy. Phys Imaging Radiat Oncol 2023;28: 100490. https://doi.org/10.1016/j.phro.2023.100490.

[42] Liu H, Schaal D, Curry H, Clark R, Magliari A, Kupelian P, et al. Review of cone beam computed tomography based online adaptive radiotherapy: current trend and future direction. Radiat Oncol 2023;18:144. https://doi.org/10.1186/s13014-023-02340-2.